Non-Interceptive Beam Current and Position Monitors for a Cyclotron Based Proton Therapy Facility

Srinivasan, Sudharsan

DOI:
10.33612/diss.149817352

Chapter 5: Prototype Tests of the Four-quadrant Dielectric-filled Reentrant Cavity Resonator as a Proton Beam Position Monitor (BPM)

5.1 Introduction

In the previous Chapter, the design of a non-invasive cavity beam position monitor (BPM) based on the dipole (TM_{110}) mode excitation has been described. It is important to compare the simulated estimation of the expected position sensitivity of the BPM and a test-bench characterization prior to its installation in the beamline. In this Chapter, the test-bench characterization of the cavity BPM is described. The test-bench results are compared with the simulation results to identify and correct for sources of error (RF interference, impedance mismatch, cavity asymmetries). As a result, the test-bench results after implementing corrections for the errors provides confidence in the signal estimate and the properties of the cavity. Following which, beamline measurements of the cavity BPM are performed for proton beam energies of 200 MeV and 138 MeV for the beam current in the range 0.1-15 nA.

5.2 Purpose of a test-bench

The test-bench that is used to characterize the BPM is the same as that was used for the characterization of the BCM. The definition of the S-parameter measurements and the description of the test-bench can be found in Chapter 3. The only component that is different in this test-bench characterization is the Device Under Test (DUT), which is the BPM.

The BPM is constructed as a combination of four cavities that are suspended by insulators within a common ground cylinder made of aluminum. The four aluminum cavities are designed in the configuration of an LC resonator. These four cavities have a common dielectric in their capacitive part made from 99.5% alumina. The insulators that keep these cavities floating within the ground cylinder are made from PEEK.

The test-bench characterization of the BPM is performed under two schemes of S-parameter measurements:

- With a beam analogon, i.e., a stretched wire, to evaluate individual cavity position sensitivity from the $S_{(beam - pickup)}$ measurements.
- Without a beam analog, to validate the cavity characteristics of the BPM, such as the resonance frequencies of the excited modes and the mutual pickup coupling S-parameters.

5.3 S-parameter measurements

As mentioned in Chapter 3, the S_{ji} is the reflection (when j=i) or transmission coefficients of a multiport device under test (DUT), in this case, the BPM, as a function of frequency. As seen in the previous Chapter, the $S_{beam - pickup}$, given in dB, of a given pickup, is a minimum for negative displacements (beam position shifted away from the cavity) and a maximum for positive displacements (beam position offset towards the cavity). With increasing negative displacements, the minimum of the $S_{beam - pickup}$ moves to higher frequencies. However, for increasing positive displacements, the maximum of the $S_{beam - pickup}$ is not shifted in frequency. Hence, the position sensitivity of individual cavities is measured only for positive beam displacements (i.e., for each cavity, the beam analogon moves towards the cavity) in the test-bench. In Figure 5.1, the relation between the displacement and the cavity used for the measurement is indicated. The $S_{beam - pickup}$ measurements for the cavities are performed individually with a center frequency of 145.7 MHz and a span of 60 MHz.

As described in subsection 4.3.2, the beam position information is directly available from the individual cavity signals. For example, as shown in Figure 5.1, the X1-signal for a beam displaced to the left and the X2-signal for a beam displaced to the right. It is essential to remember that the position information is not provided by the difference of the X-plane (Y-plane) cavities. All transmission measurements are performed with an accuracy < 0.05 dB for frequencies above 9 kHz [1]. This corresponds to the pickup voltage accuracy < 0.5%.

NOTE: In our tests, position sweeps in X-axis are for zero position of the Y-coordinate and vice-versa.

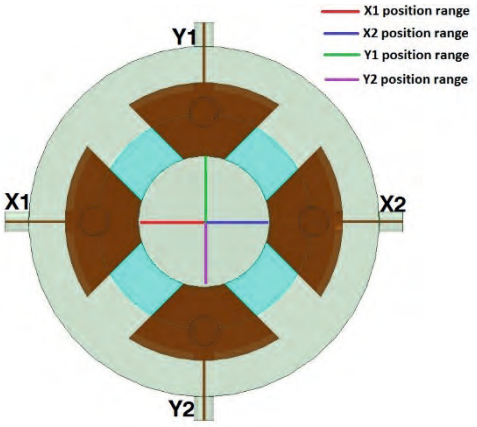

Figure 5.1: Reference for S_{ji} measurement of individual cavities with respect to beam entrance port (into the page). The arrows represent the domain for beam position-offset for measurement of individual cavities (as positive displacements). Color reference for the image can be found in Figure 4.5.

5.3.1 $S_{beam\text{-}pickup}$ measurements

The S-transmission measurement (S_{ji}) is performed where i represents the source port (beam entrance port) and j represents the receiver port (cavity pickup loop port terminated with $50\,\Omega$). The measurement results are summarized and are compared with the simulation, as shown in Figure 5.3. The measured TM_{110} mode resonance frequency is for all the cavities, 145.7 MHz, which is the design requirement. Also, the other modes i.e., the TM_{010} (monopole) mode and the higher-order mode, TM_{210}, show a good agreement at the simulated frequencies: 127.5 MHz and 152.5 MHz.

The important observations are summarized as:

- The absolute signal level of the zero position information, which is the TM_{010} mode amplitude of the cavity, is 12 nV lower than the simulation.
- With increasing position offset the difference in amplitude between measurement and simulation increases to approximately 30 nV for a position offset of 15 mm. The average measurement sensitivity is lower by approximately 58% as compared to the simulation.
- The absolute signal levels of the cavities differ with respect to each other (4%-6%). This is due to differences in the machining and assembly tolerances of the individual cavities, which cannot be avoided. This difference in signal level of the individual cavities with respect to each

other is within the tolerance limit of the dimensions defined from the simulation design.

The reasons for the observed deviation between simulation and measurement for both position sensitivity and signal level could be the following:

- Spurious RF interference affecting the signal strength observed in the test-bench thus affecting overall signal sensitivity.
- Existence of impedance mismatch of the beam entrance port [2].
- Asymmetries in the cavity BPM such as cavity translation, dielectric translation error, or rotational asymmetries. These asymmetries could be a combination of two or more and present in one or more of the floating cavities.

Corrections for the above-discussed reasons are implemented by the following:

- The RF interference is minimized by isolating the beam analog (stretched copper wire) by covering the whole test-bench setup with aluminum foils.
- The impedance mismatch is corrected by providing a ground connection for the hanging stretched wire.
- The cavity BPM system is reassembled following a metrological inspection to correct for asymmetries.

The result of the above implementation is given in the following section.

NOTE: The cavity asymmetries are intrinsic due to the complex mechanical assembly, of which, specific commonly occurring asymmetries are discussed in subsection 4.4.3.

5.3.2 Conclusion on sensitivities

The observed difference in absolute signal level for position offsets and position sensitivities of individual cavities could be a combination of the above-discussed asymmetries, impedance mismatch and the RF interference in the lab environment.

After reassembly and the implemented corrections (ground connection and RF interference isolation), we observed a shift of the resonance frequency of the TM_{110} mode in the X- cavities and in the Y-cavities to 146.0 MHz and 148.1 MHz, respectively. The shift of the TM_{110} mode resonance frequency by 2.4 MHz for Y-axis cavities is equivalent to a too-small reentrant gap radius of approximately 1.6% (1.4 mm reduction in the reentrant gap radius). For the X-axis cavities, since the shift in their TM_{110} mode resonance frequency

(146.0 MHz) closest to the design frequency of 145.7 MHz, the XX crosstalk is used as a reference.

In Figure 5.2, the S_{ji} (between two X-axis cavities, i.e., XX crosstalk) in the absence of stretched wire measured before and after reassembly is compared with simulations. These indicate the sensitivities in practice, the effects of the above-mentioned corrections in the reassembled cavity BPM.

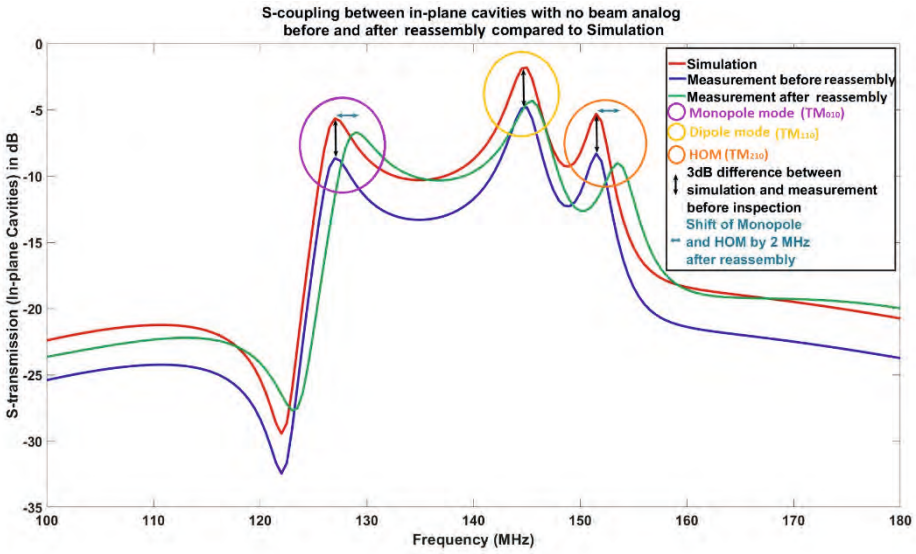

Figure 5.2: S_{ji} for in-plane cavities (X-axis) before and after reassembly (and corrections) (with no beam analog) compared with simulation. Marked in circles are the modes that can be excited in the structure between 100-180 MHz. Port *j* and port *i* represents the pickup loop ports of the two X-axis cavities.

In addition, the influence of the prototype reassembly and the corrections (for impedance mismatch and RF interference) on XX crosstalk is clearly seen. Prior to the reassembly and corrections, the frequencies of all the excited modes within the span of 100-180 MHz were in good agreement with the simulation results. The measured coupling coefficients (strength) of these TM modes were, however, lower by approximately 3 dB as compared to the simulation. After reassembly and the corrections, the coupling between the two in-plane cavities (for the TM_{010} and the TM_{110} modes) is enhanced but still short of the simulation results. On the contrary, the strength of the TM_{210} mode at 152.5 MHz is weakened. Concurrently, the TM_{010} mode is shifted closer to and the TM_{210} mode is farther from the TM_{110} mode by 2 MHz, which in itself is shifted by 300 kHz

approximately. These observations provide an insight into the role of cavity asymmetries on modes that can exist in the frequency domain 100-180 MHz.

The S-transmission parameters between the beam entrance and each individual cavity are measured on the test-bench after reassembly and the results are summarized in Figure 5.3 and Table 5.1. The position sensitivity of the X-plane cavities and the Y-plane cavities are measured at 146.0 MHz and at 148.1 MHz, respectively, to provide position sensitivity at the maximum of the dipole mode excitation. The position sensitivity of the X-plane cavities (TM_{110} mode resonance frequency at 146.0 MHz), when measured at 145.7 MHz, is reduced by approximately 10%. The position sensitivity of the Y-plane cavities (TM_{110} mode resonance frequency at 148.1 MHz) if measured at 145.7 MHz is reduced by approximately 92%.

Table 5.1: Comparison of S-transmission for individual cavities corresponding to positive displacements between simulation and measurements after the reassembly (and corrections). Cavity voltage represented in nV for 1nA beam current equivalent.

Offset	**(nV)**	**(nV) X-axis 146.0 MHz**		**(nV) Y-axis 148.1MHz**	
(mm)	**HFSS**	**X1**	**X2**	**Y1**	**Y2**
0	16.2	17.9	17.0	13.2	14.5
2	20.5	20.8	19.7	16.2	17.5
5	27.5	26.0	24.5	20.6	22.5
10	38.7	35.3	32.8	28.7	32.9
15	49.7	44.7	41.4	36.9	42.4

Figure 5.3 shows that the absolute signal level of the individual cavities and their position sensitivity are in reasonable agreement with the HFSS simulation results after the reassembly and corrections. To indicate the effects of these, also the data taken before are shown here. The average signal level for the zero position (of the four cavities) is approximately 15.6 nV. This represents the amplitude of the TM_{010} mode at the resonance frequency of the TM_{110} mode. This is within 5% of the simulation value. Similarly, the average of the absolute signal level at every position offset is increased. For instance, at the 15 mm position offset from the center, the average signal level is 41.5 nV, which is 23 nV higher than the measurement before reassembly and corrections but is still approximately 16 % less than the simulation value. Although the reassembly and corrections have

improved the sensitivities significantly, the position sensitivities of the individual cavities are still lower than the simulation value and different with respect to each other. This difference between the simulation and the measurement might be due to the relatively high loss-factor of the alumina ring compared to the loss-factor of $2x10^{-4}$ assumed in the simulation as we observed in the simulation with different loss-factors.

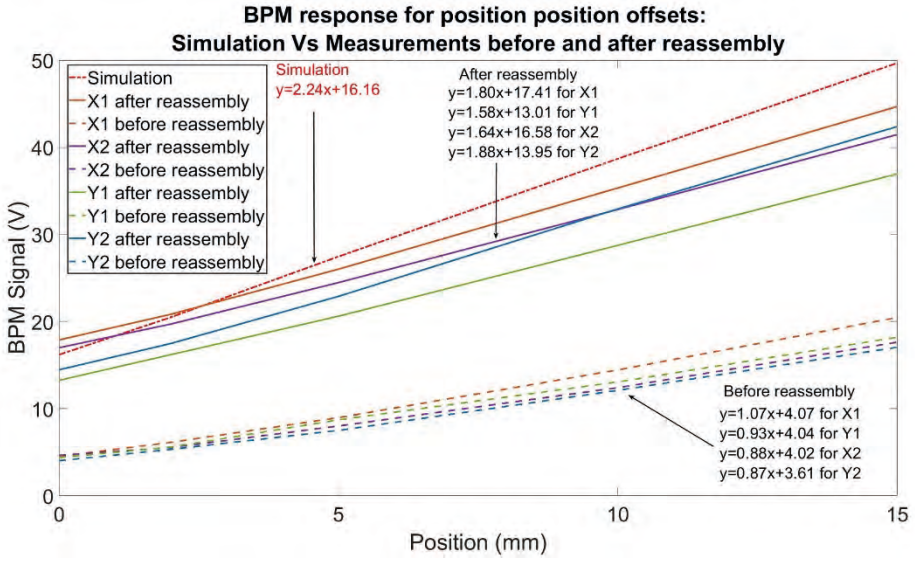

Figure 5.3: S-transmission for individual cavities as a function of position offset (stretched wire moving towards cavity). The simulation (dot-dash line) and the measurements before (dashed lines) and after (solid lines) reassembly and corrections are shown. Before the inspection, the TM_{110} mode resonance frequencies of the cavities were matched to 145.7 MHz but had a lower signal level. After reassembly and corrections, the signal level is comparable to the simulation at the expense of frequency shift in the X-plane to 146.0 MHz and in the Y-plane to 148.1 MHz.

5.4 Beamline measurements

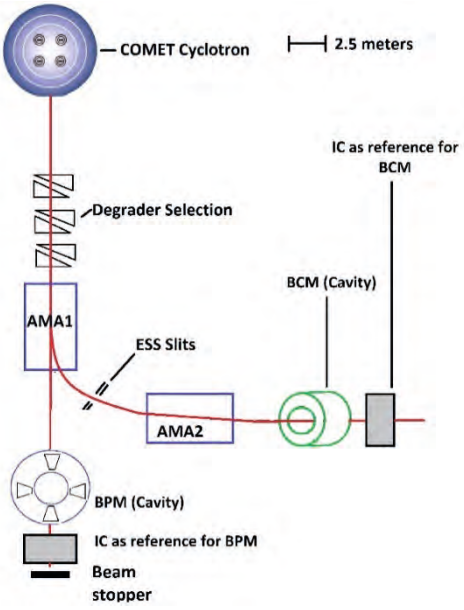

Figure 5.4: BPM prototype installation in the beamline. Located at approx. 12 meters from the Cyclotron exit (6 meters from the degrader exit).

This section summarizes the beam position measurements with the BPM using a real beam from the cyclotron following a second reassembly prior to beamline installation. The second reassembly was performed to shift the TM_{110} mode resonance frequency back to 145.7 MHz without much compromise on the XX crosstalk coefficient. However, the second reassembly resulted in shifting the TM_{110} mode resonance frequency of the X-axis by 100 kHz to 146.1 MHz and the Y-axis by 700 kHz to 148.8 MHz, as a result of more asymmetry effects. The X-axis cavities are chosen for in-beam measurement validation since their TM_{110} mode resonance frequency is closest to 145.7 MHz. The Y-plane cavities were not used in the measurements because of the offset of their resonance frequency by approximately 3.1 MHz from 145.7 MHz. The beam-pickup coupling was not measured in a test-bench environment after the second reassembly since the XX crosstalk measured on the installation platform did not differ drastically from the results after the first reassembly. Moreover, the measurements only aim at validating the monitoring of beam position of low-intensity proton beams. From these measurements, we expect more insight into the optimization of the BPM performance through design modifications. The BPM prototype is installed at 6 meters from the degrader exit, as shown in Figure 5.4. Therefore, the difference

in the bunch length for different energies is expected to be minimal, unlike for the BCM measurements discussed in Chapter 3.

The measurement reference for beam intensity and position is a multi-strip ionization chamber (IC), which is located within a meter behind the BPM. The beam position measurements are performed individually for each X-axis cavity with 50 Ω termination on the pickup loops of the unused X and Y-axis cavities. The measurement chain is as represented in Figure 5.5 and data acquisition was performed with a handheld spectrum analyzer (single-channel measurement, instrument limitation) from Rohde and Schwarz FSH8 [3]. The first stage amplification consists of four Low-Noise Amplifiers (LNAs) for each cavity; two with 30 dB (Y-plane cavities) amplification and two with 36 dB amplification (X-plane cavities). A common-mode choke, i.e., Balanced to Unbalanced (BALUNS) [4] was used for the power supply of the first stage amplification, which helps in resolving ground loop problems and reduces the RF interference from power supply lines.

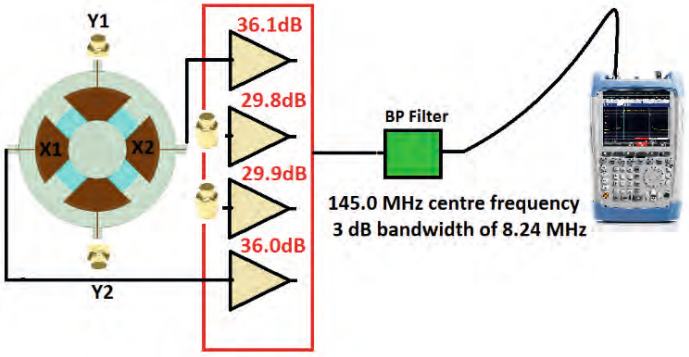

Figure 5.5: Measurement chain for the BPM measurement. The amplification box (in red) consists of 4 LNA (50Ohm: 36.1; 29.8; 29.9; 36.0 dB). The measurement is performed with a handheld spectrum analyzer from Rhode and Schwarz (FSH8 model). The bandpass filter is with a center frequency of 145.0 MHz 3 dB bandwidth of 8.24 MHz. Color reference for the cavity BPM image (left) can be found in Figure 4.5.

The first stage of the measurement involves validating the operational principle of the BPM prototype on the basis of beam current response for two given offset positions (positive displacements): 2.4 mm and 4.8 mm at 200 MeV proton energy. In addition, measurements were performed by sweeping the beam current at two different energies: 138 MeV and 200 MeV at a position offset of 4.8 mm to check the influence of energy spread on the resonator's beam intensity response for a given position offset. The position offset used for characterization is a

positive displacement, i.e., the beam towards the measuring cavity, because the polarity of the TM_{010} mode and the positive polarity of the polarization of the TM_{110} mode (for positive displacements) are then in the same direction.

The second stage of the measurements involved sweeping the beam's position in the X-plane (zero Y-coordinate of the beam) to estimate the position sensitivity of the individual X-axis cavities. The position measurement is performed at 138 MeV for two different intensities: 2.6 nA and 12.2 nA.

NOTE: All the measurements are recorded in units of dBm with the handheld spectrum analyzer. The measurement uncertainty of the spectrum analyzer is ±0.05 dB. The reference beam current and position measurements are recorded with an IC with uncertainty of 1% (for beam current) and 5% (for beam position).

5.4.1 Beam current response

200 MeV: Beam current sweep at position offsets: 4.8 mm and 2.4 mm

The measurement-offset (or "no-beam response") of the X1 cavity at 145.7 MHz was measured, prior to the beam current measurement, with the cyclotron RF turned on, but with no beam in the beamline. This measurement-offset is a combination of RF interference from the cyclotron, background noise, voltage fluctuations at the input of the first-stage amplifier from the ground loop and other spurious interferences from radio communications in the frequency band 144-146 MHz [5]. The amplitude of the measurement-offset from the X1 cavity was measured as 4.6 μV and was observed to remain essentially constant over a duration of a few seconds.

The measured data of the X1 cavity are offset-corrected (by subtracting the measurement-offset), under the assumption that the measurement-offset and the beam-induced signal from the X1 cavity are in phase. Under this assumption, the X1 cavity behavior with respect to beam current is studied. Thenceforth, the offset-corrected data is normalized to beam current to determine the average signal for a given position offset.

The 200 MeV proton beam is swept over a range of 0.1-15 nA at two different positions: 4.8 mm and 2.4 mm towards the X1 cavity. The X1 cavity response with measurement-offset correction and beam current-normalisation is shown in Figure 5.6.

In Figure 5.6 (a), we observe the linear behavior of the X1 cavity response as a function of beam current at the two position offsets. It is important to validate this linear relationship since the BPM response is a function of both the beam current

and position. By normalizing the X1 cavity response (Figure 5.6 (a)) with respect to beam current, we achieve a nearly constant response of the X1 cavity, within a relatively large uncertainty range, as shown in Figure 5.6 (b).

NOTE: The error bars of the normalized BPM response (Figure 5.6 (b)) indicate $\pm 2\sigma$ uncertainty and the confidence interval of the mean normalized value is $\pm 1\sigma$.

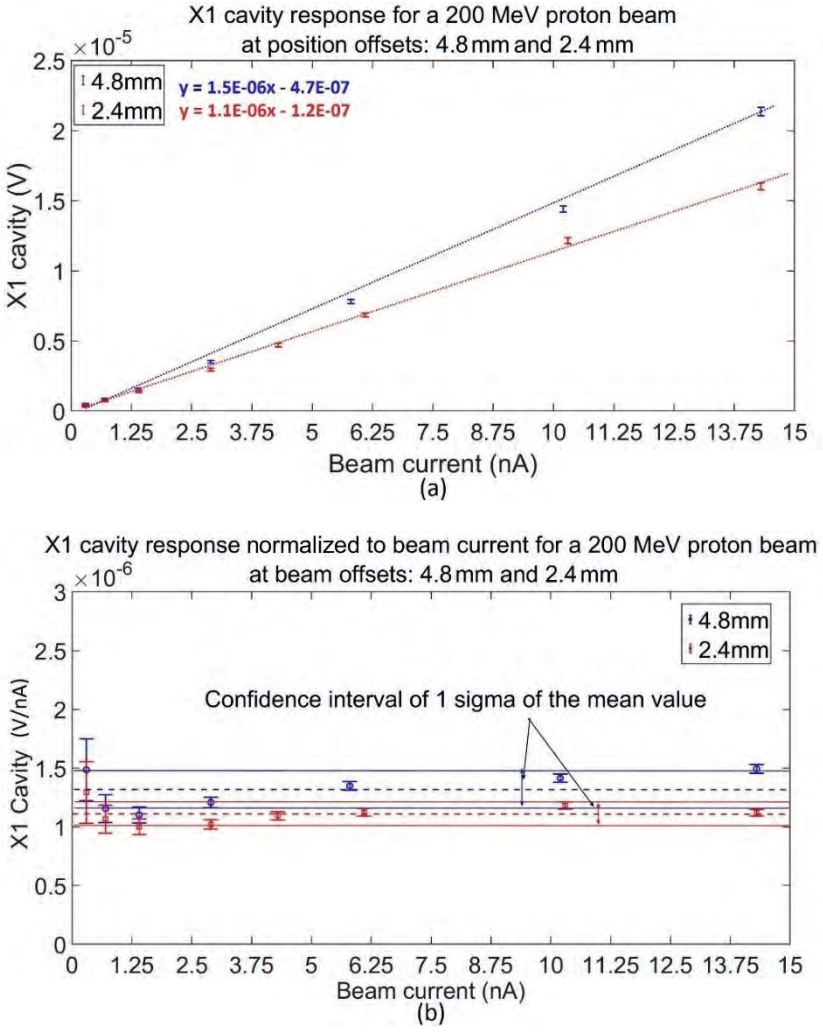

Figure 5.6: Shown in (a) is the X1 cavity response with measurement-offset correction for a 200 MeV proton beam at beam positions: 4.8mm and 2.4mm towards X1. Shown in (b) is the beam current-normalized response. The error bars of individual data points shown in both the plots constitute two σ measurement uncertainty.

200 MeV and 138 MeV: Beam current sweep at position offset: 4.8 mm

The measurement was repeated at an energy of 138 MeV for a beam offset of 4.8 mm towards the X1 cavity. The X1 cavity response with measurement-offset correction and beam current-normalization is shown for 138 MeV and 200 MeV in Figure 5.7.

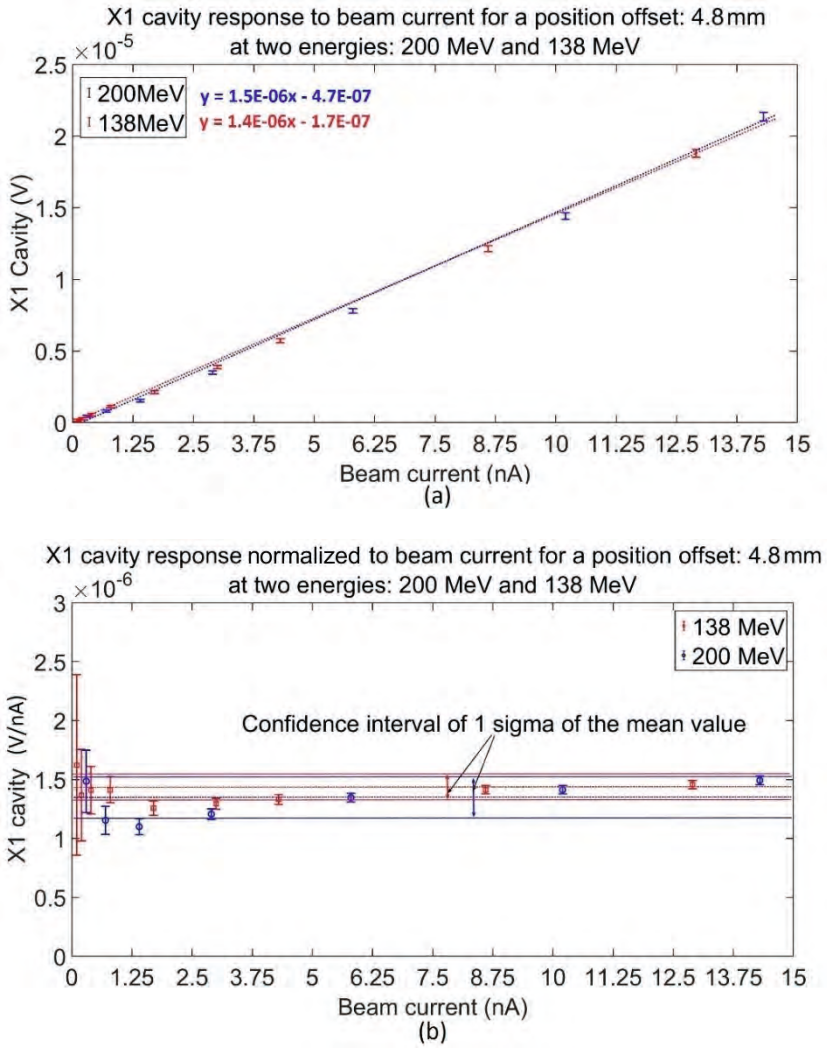

Figure 5.7: Shown in (a) is the X1 cavity response with measurement-offset correction for a 200 MeV and 138 MeV proton beam at 4.8mm towards X1. Shown in (b) is the beam current normalized response. The error bars of individual data points shown in both the plots constitute two σ measurement uncertainty.

Since the BPM is installed in the beamline at six meters from the degrader exit, there is only a minimal difference (4%) of the bunch length at the two different energies. The beam current sensitivity of the BPM (X1 cavity) given by the slope of the curve is lower by only 3% at 138 MeV compared to 200 MeV. This is in good agreement with the expected small difference in bunch length.

Normalizing the BPM response (X1 cavity after offset correction) by correcting for the beam current provides the position related signal sensitivity of the BPM, which is expected to be constant as a function of beam current. This should not differ for different beam energies and this is clearly shown in Figure 5.7 (b) but within a relatively large uncertainty range. Similar to the observation in the previous measurement, there is a drop in sensitivity for beam currents ≤ 2.5 nA.

NOTE: The error bars of the normalized BPM response (Figure 5.7 (b)) cover ±2σ uncertainty and the confidence interval of the mean normalized value is ±1σ.

- *Discussion*

In both Figure 5.6 (b) and Figure 5.7 (b), the normalized response (with respect to beam current) of the BPM's X1 cavity, after measurement-offset correction, shows a drop in sensitivity for beam currents ≤ 2.5 nA.

A possible explanation of this sensitivity drop with decreasing beam intensity is shown in Figure 5.8, where vectors $\vec{A}, \vec{B}$ and $\vec{R}$ represent measurement-offset, beam-induced BPM response and measured response, respectively.

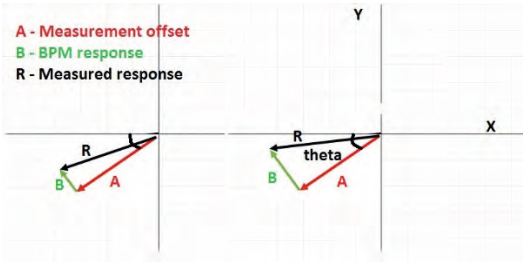

Figure 5.8: An example vector representation of the measurement scenario. The vectors indicating the time-dependent amplitudes and phases of A represent the measurement-offset, of B represent the BPM response and of R represent the resultant vector and theta is the orientation of the measurement-offset. Vector B is assumed in this scenario to be at 90° with respect to A. The left represents the scenario for small beam current at a given offset and the right represents for large beam current values. Variations in the magnitude of vector A affects the magnitude of vector R relatively strongly when vector B magnitude is small compared to large vector B magnitude.

In this example scenario, the BPM response $\vec{B}$ is at 90° with respect to the measurement-offset. The left schematic is for small beam currents and the right schematic for large beam currents for a given beam position offset. For a smaller magnitude of vector $\vec{B}$, the magnitude of the resultant $\vec{R}$ is influenced relatively strongly by variation in magnitude of vector $\vec{A}$ compared to a larger magnitude of vector $\vec{B}$. The relative phase between the BPM response $\vec{B}$ and the measurement-offset $\vec{A}$ thus needs to be taken into account when correcting for the measurement-offset. This is an important observation that needs to be taken into account while designing the measurement chain for the BPM. The spectrum analyzer that was used in the measurement does not have that possibility, however. It is therefore recommended to have a measurement-offset vector correction through I/Q demodulation [6] of the signal from the BPM with respect to the RF of the cyclotron.

5.4.2 Beam position response

In the previous subsection, we measured the BPM's X1 cavity response as a function of beam current. In this section, the position response of the X-axis cavities (both X1 and X2) is measured for a 138 MeV proton beam. The full width at half maximum (FWHM) of the proton beam was measured as 20 mm in both X and Y planes. The measurement is divided into two parts:

- Beam position sweep in X-axis to determine the position sensitivity of the X-axis cavities. The beam is swept in position across the X-direction at two different beam currents: 2.6 nA and 12.2 nA. The Y-coordinate of the beam was kept constant at 1.05 mm.
- X2 cavity measurement for beam position sweep in the Y-direction to validate the non-excitation of the horizontal polarization in the dipole mode. The X coordinate of the beam was kept constant at 0 mm.

X-axis sweep

A 138 MeV proton beam is swept in position in the X-direction for a fixed Y-coordinate of the beam. The Y-coordinate of the beam centroid (1.05 mm) was chosen as close to zero as achievable. The position measurement is performed at two beam intensities: 2.6 nA and 12.2 nA. From the previous section, it was concluded that the lowest beam current for which a reliable response from the cavities could be measured with the help of the existing measurement chain is about 2.6 nA. The zero position information of the individual cavities (X1 and X2), which includes the measurement-offset and the TM_{010} mode amplitude at the

TM_{110} mode frequency, is subtracted from the measured position response for displacements of the beam towards the cavities. The corrected response of the cavities is given by normalizing for beam current after zero position information is subtracted. The corrected response of the cavities from the measurement results are plotted in Figure 5.9.

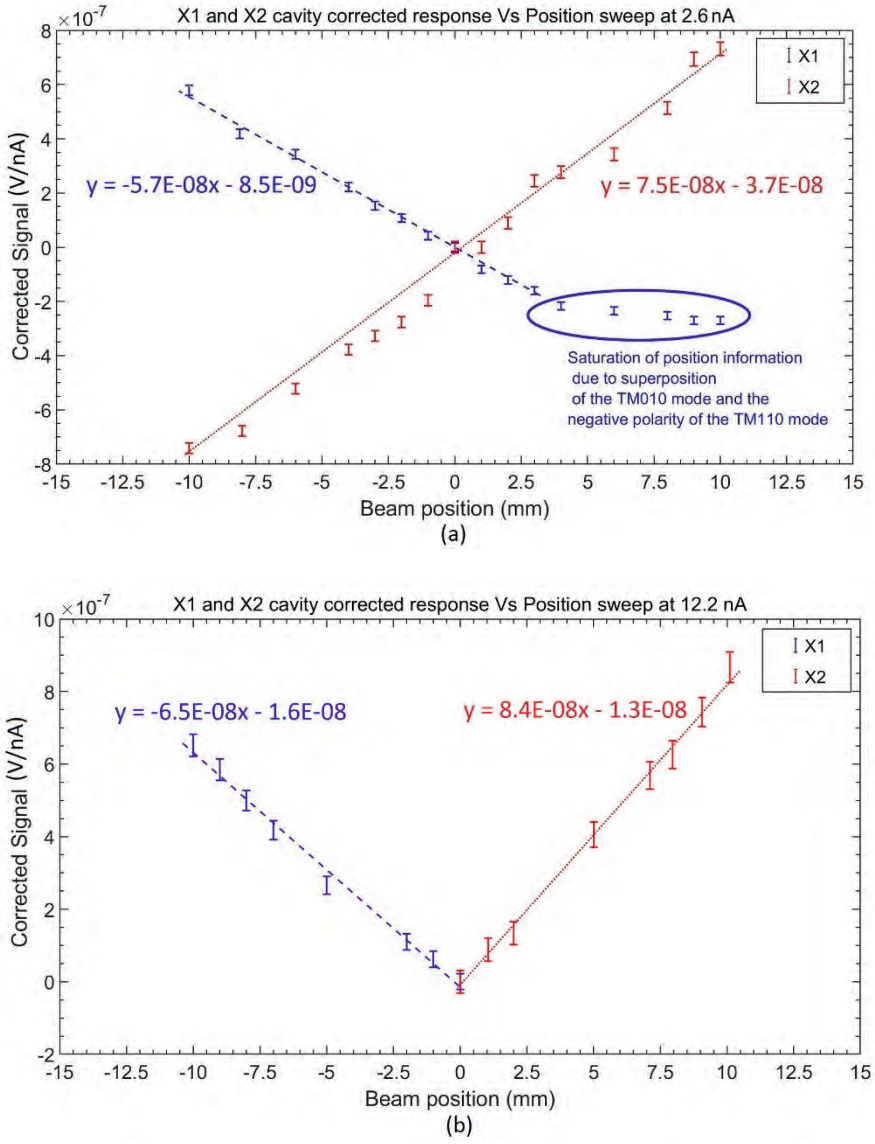

Figure 5.9: X1 and X2 cavity signal after measurement-offset correction and beam current normalization plotted Vs beam position (X-axis sweep). The data points are plotted with a 95% confidence interval (±two σ uncertainty). (a) represents for beam current = 2.6 nA and (b) represents for beam current = 12.2 nA. Reference beam current and position are measured with a profile monitor with fractional uncertainty is 1% and 5% respectively.

The beam moving towards the left is a positive offset for X1 cavity and the beam moving towards the right is a positive offset for the X2 cavity. The reference (X, Y) coordinate is defined for a beam entering the page in Figure 5.5.

NOTE: For a beam current of 2.6 nA, the position sweep is performed for a range of - 10 mm to +10 mm for both the cavities. For a beam current of 12.2 nA, the position -10 mm to 0 mm for X1 cavity and from 0 mm to +10 mm for X2 cavity.

Y-axis sweep

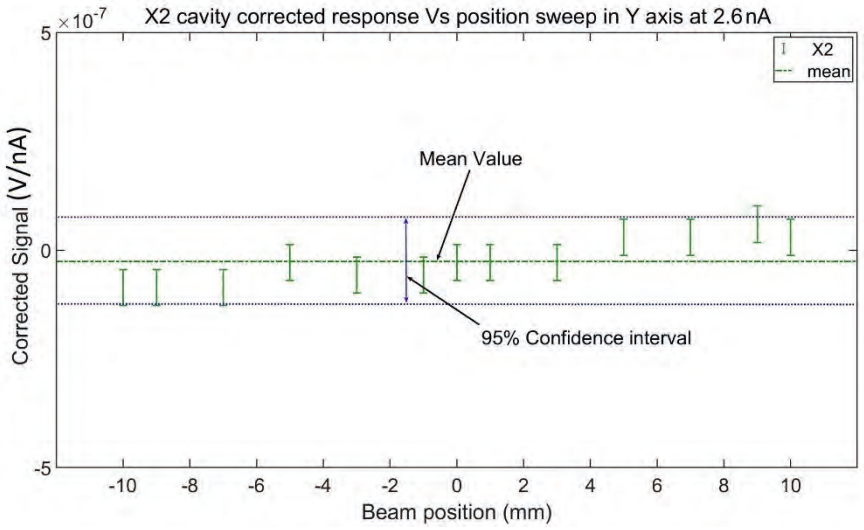

Figure 5.10: X2 cavity signal after measurement-offset correction and beam current normalization plotted versus position in Y-axis over a range -10.0 mm to +10.0 mm. Each data point is plotted with a 95% confidence interval (±two σ uncertainty). The green line represents the average of the measurement and the blue lines represent the two σ uncertainty.

The beam with an intensity of 2.6 nA was swept along the Y-axis from -10.0 mm to +10.0 mm. The X2 cavity response after measurement-offset correction and beam current normalization is shown in Figure 5.10. For a pure translation along the Y-axis, the TM_{110} mode's horizontal polarization of the cavity is expected not to be excited. Consequently, the signal of the X2 cavity should not depend on the Y-position. The measured signal is due to the TM_{010} mode of the cavity as it is the position-independent mode.

- *Measurement results from 2.6 nA position sweep*

The linear fit equations from Figure 5.9 is given by

$$\begin{aligned} X1\ Cavity &= M1\,X - C1 \text{ where } M1 = -5.7\text{E-}8 \text{ V/mm}, C1 = 8.5\text{E-}9 \text{ V} \\ X2\ Cavity &= M2\,X - C2 \text{ where } M2 = 7.5\text{E-}8 \text{ V/mm}, C2 = 3.7\text{E-}8 \text{ V} \end{aligned} \quad (5.1)$$

where, X (in mm) represents the negative displacement for the X1 cavity (- 10.0 mm to 0.0 mm) and represents positive displacement for the X2 cavity

(0.0 mm to +10.0 mm). The position sensitivity of the X1 cavity (M1) has a standard deviation of 3%, while for the X2 cavity (M2), the standard deviation is 6%. The inverse of the slopes provides the position calibration factor of the cavities, which are needed to calculate the displacement from the BPM measurement data.

The position error is given by the average of the absolute difference between the reference position and the position calculated. The measurement error is composed of a systematic part, which includes the alignment offset, the measurement-offset, and a stochastic part. The stochastic uncertainty is given by the standard deviation (1σ) of the calculated position. The position error and uncertainty of the X1 and X2 cavities are given as

$$\begin{aligned} &\text{X1 CalPosition error} \pm \text{uncertainty} = 0.21\ \text{mm} \pm 0.17\ \text{mm} \\ &\text{X2 CalPosition error} \pm \text{uncertainty} = 0.54\ \text{mm} \pm 0.26\ \text{mm} \end{aligned} \tag{5.2}$$

- *Measurement results from 12.2 nA position sweep*

The position error and the uncertainty of the X1 and X2 cavities derived from measurements with 12.2 nA beam current is given as

$$\begin{aligned} &\text{X1 CalPosition error} \pm \text{uncertainty} = 0.27\ \text{mm} \pm 0.18\ \text{mm} \\ &\text{X2 CalPosition error} \pm \text{uncertainty} = 0.18\ \text{mm} \pm 0.14\ \text{mm} \end{aligned} \tag{5.3}$$

The signal-to-noise ratio (SNR) of the measurement is expected to increase with higher beam currents. Consequently, this should reduce the measurement error for measurements with higher beam currents. For the X2 cavity, the position uncertainty is better by a factor of three for measurements with 12.2 nA as compared to measurements with 2.6 nA. For the X1 cavity, we do not observe the same behavior. The difference of 0.06 mm in the position error is within the resolution limits of the X1 cavity. This might be due to the measurement instrumentation limitation and might be due to varying amplitude of the measurement offsets during the course of these experiments, as we observed. With a dedicated measurement chain, we expect to minimize such effects.

- *Discussion*

In Figure 5.9, the difference in position sensitivity between X1 and X2 cavity is approximately 29% for measurements with beam current at 12.2 nA and is 32 % at 2.6 nA. This difference in position sensitivity between two cavities should not depend on the beam current. Since the comparison is between a relatively low and high beam current, the observed difference could be due to the influence of

the measurement-offset, especially for the 2.6 nA beam current measurement as indicated in Figure 5.8.

The higher position sensitivity of the X2 cavity compared to the X1 cavity could be due to induced asymmetries after multiple reassembles. This could have resulted in affecting the $S_{beam\text{-}pickup}$ coefficients of the cavities such that the saturation of the position response (encircled for X1 cavity in Figure 5.9) is different for different cavities. Due to this, the response of the X2 cavity is linear over a position range of - 10.0 mm to +10.0 mm, while for the X1 cavity, it is linear over a smaller range from -10.0 mm to +3.0 mm.

The positive X displacement of the beam can be obtained from the linear fit equations of the X2 cavity and the negative X displacement from that of the X1 cavity. The position sensitivity of the X2 cavity is approximately 11% higher when measured with a beam current of 12.2 nA compared to 2.6 nA and for the X1 cavity, this is approximately 14%.

For a smaller product of beam current and position (i.e., beam current × position ≤ 2.5 nA mm), the measurement-offset are dominating the amplitude measured by the spectrum analyzer. When the product of beam current and position is larger than 2.5 nA mm, the BPM response is not influenced to a significant extent by the measurement-offset.

The measurements presented in Figure 5.10 confirm the non-excitation of the horizontal (or vertical) polarization of the dipole mode for beam position sweeps in vertical (or horizontal) direction. This is an important observation to validate the principle of operation of the BPM as expected from the simulation results. For an arbitrary (X, Y) beam position, both polarization of the dipole mode will be excited.

- *Summary of beam measurements*

With the beam current sweep and the beam position sweep measurements, we have demonstrated the ability to perform the following without disregarding the existence of a significant and fluctuating background signal. The measurement summary is as follows:

- Beam position offsets for beam currents as low as 0.1 nA (Figure 5.6 and Figure 5.7). These measurements indicate a typical sensitivity in the order of 56-75 nV/mm, and a position uncertainty of < 0.5 mm

- Beam position offsets vary linearly with position over a position range of -10.0 mm to +10.0 mm by X2 cavity and from -10.0 mm to +3.0 mm by X1 cavity as shown in Figure 5.9.
- Beam position offsets have been obtained with an average position error of 0.4 mm by X2 cavity and 0.2 mm by X1 cavity, respectively within the required specification of 0.5 mm.
- The quadrant of the beam position offset is identified without the need for a monopole cavity (as in conventional cavity BPMs) by taking advantage of mode interference and induced cavity asymmetries.
- A good agreement between the measured difference (3%) in beam current sensitivity and the expected difference (4%) due to bunch length spread has been observed.

Non-interceptive beam position measurement at PROSCAN (PSI) has been demonstrated successfully with the help of a dielectric-filled reentrant cavity, with minor adversities. The performance of a cavity BPM in terms of position sensitivity and resolution are within the specifications required for PROSCAN. These could be improved further by minimizing the measurement-offset and its fluctuations. This could be performed by measuring the complete vector instead of only the amplitude, by referencing to the cyclotron RF (phase measurements). The measurement-offset vector from the BPM cavities could be measured by performing measurements while interrupting the beam, followed by measurement with the beam through the cavity. In addition, the BPM's performance could be enhanced with design optimization, to minimize mode interference and maximize output signal for a given position offset. In the following section, the expected performance of a new version of the BPM design is discussed.

5.5 New version of the BPM Design: Overview

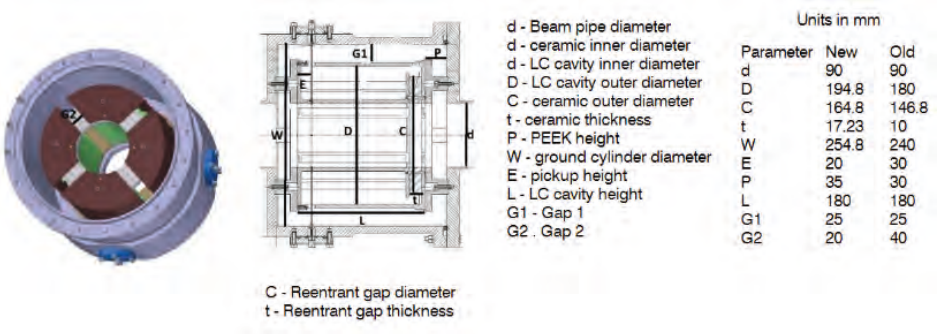

Units in mm

Parameter	New	Old
d	90	90
D	194.8	180
C	164.8	146.8
t	17.23	10
W	254.8	240
E	20	30
P	35	30
L	180	180
G1	25	25
G2	20	40

Figure 5.11: Cut-plane of the New BPM design modified with the help of ANSYS HFSS parametric investigation. Marked are the relevant dimensions of the new BPM.

In the previous sections, the successful demonstration of non-invasive beam position measurement with a four-quadrant dielectric-loaded cavity resonator system has been described. The position sensitivity and the signal level can be enhanced by optimizing the design. ANSYS HFSS is used to optimize the design parameters based on the sensitivity analysis reported in Chapter 4. A major drawback of the existing BPM prototype is the presence of cavity asymmetries and the low loaded quality factor of the TM_{010} and TM_{110} modes. The asymmetries are minimized in the new design by providing PEEK support plates instead of PEEK rings as in the existing BPM prototype. The design parameters are optimized such that the loaded quality factors of the TM_{010} and TM_{110} mode are increased and the modes are separated further in the frequency domain than in the prototype. This combined effect is expected to minimize the presence of the TM_{010} mode at the TM_{110} mode frequency but only to a level such that the constructive interference of the TM_{010} and the TM_{110} modes still allows determining the beam offset sign. The new BPM design is as shown in Figure 5.11.

The output voltage of the BPM for position offsets and the position sensitivity is expected to increase due to the modifications shown in Figure 5.11. The modifications in the new design include:

- Increase in the reentrant gap of the floating cavities by approximately 8% and the reentrant gap thickness by approximately 72%.
- Reduction in the gap capacitance by approximately 18% compared to the prototype.

- Increasing the azimuthal coverage from 62% of the available in the prototype to 82% of the available in the new design. This results in an increased horizontal-vertical coupling, which is compensated by the increased capacitance of the individual cavities with respect to the ground cylinder.
- The pickup height is lowered by 10 mm in the new BPM with respect to the prototype.
- The overall length of the new BPM is 1 cm longer than the prototype.

These changes have resulted in the following improvements of the operation parameters:

- Increased $(R/Q_o)_{110}$, (i.e., normalized shunt impedance) by approximately 58% such that the normalized shunt impedance of the new BPM is 23 Ω compared to 14.5 Ω of the BPM prototype by increasing the gap thickness to gap radius ratio (l/R_{res}).
- As a consequence, B_c, (i.e., beam coupling coefficient) is reduced by approximately 8% with the increase in the reentrant gap radius.
- The induced voltage within the new BPM for a given beam position offset is increased by approximately 45% due to the changes in the design of the BPM
- The output signal level for a 2 mm position offset is a minimum 3 dB higher in than the prototype for the same position offset.
- The loaded quality factor of the new BPM design compared to the prototype is increased by a factor of 7, by the above changes and by lowering the pickup height by 10 mm. The loaded quality factor (of the dipole mode) of the new BPM design is 317.

The S-parameter results of the new BPM design for position offset up to 15 mm are represented in Figure 5.12. The TM_{010} mode of the new BPM design is at 119.9 MHz and the TM_{210} mode is at 157.4 MHz.

In the new BPM design, the frequency separation between the monopole and dipole mode is 25.8 MHz, which is an increase of 7.2 MHz compared to the existing prototype. The TM_{210} is shifted from the dipole mode by 11.7 MHz, which is an increase of 5.3 MHz compared to the prototype. The new BPM design has its XY crosstalk at 11.2 dB, approximately 3 dB lower than the prototype. As a result, the transfer impedance of the BPM cavities (for position offset) compared to the prototype is improved by 15% for a 2 mm beam position, which increases up to 44% for a position offset of 5 mm. Moreover, the signal level for a centered

beam is reduced by 25%, which results in the improvement of the position sensitivity by factor of 2.4 approximately.

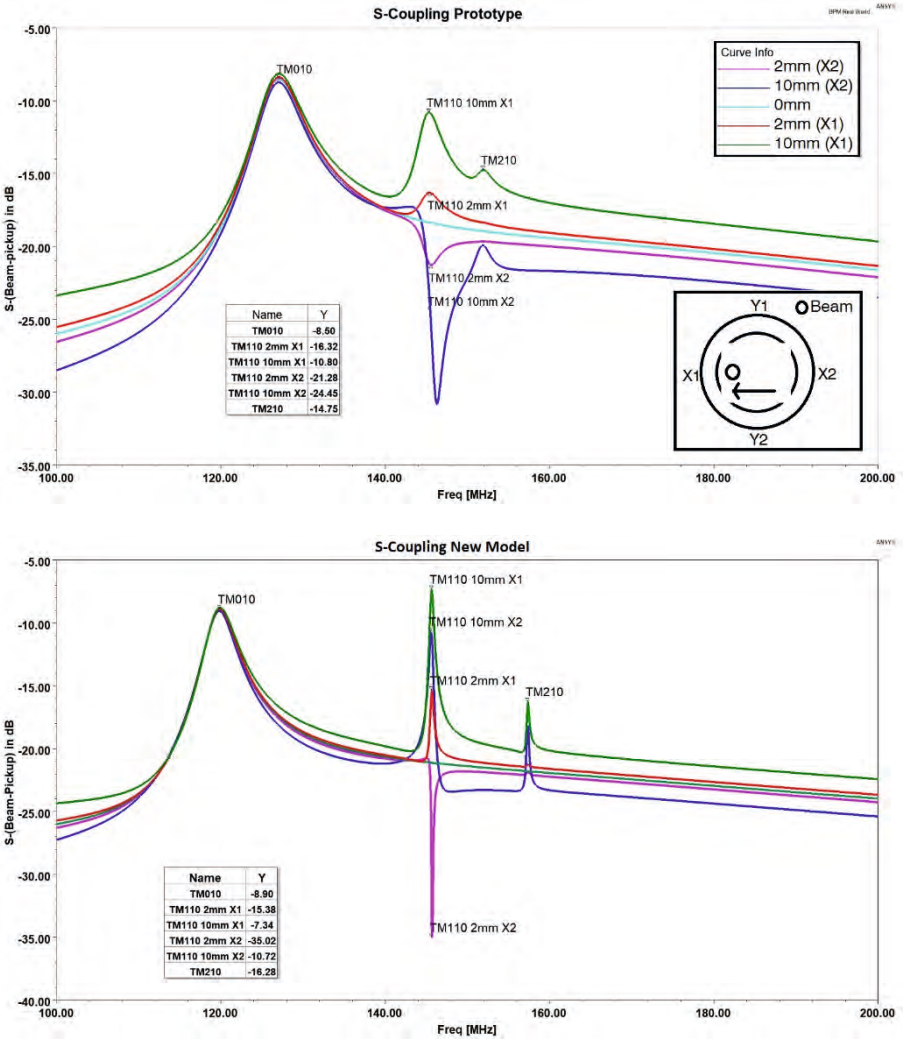

Figure 5.12: S-(Beam-Pickup) in dB for position offsets up to 10mm. Marked are the excited modes of the new BPM within a span of 100-200 MHz. The monopole mode (TM_{010}) is excited at 119.90 MHz, dipole mode (TM_{110}) at 145.70 MHz and the HOM (TM_{210}) at 157.40 MHz.

NOTE: The new BPM design has been characterized on the test-bench and is in close agreement with simulation expectations. The new BPM is expected to be validated with in-beam measurements after September 2020. Thus, its performance is not documented in the thesis.

5.6 Summary

This Chapter describes the experimental validation of the BPM prototype, both on the test-bench and in the beamline. The test-bench characterization is executed with and without a beam analog to evaluate position sensitivity of the individual cavities, to identify the excited modes within the frequency span of 100-200 MHz and to measure the XX and XY crosstalk.

The first test-bench characterization of the prototype showed that the position sensitivities of the cavities were approximately 50% lower than the simulated values. The potential reasons for the observed deviation were identified as spurious RF interference, impedance mismatch arising from problematic ground loops and minute cavity asymmetries. Following an investigation of cavity asymmetries, we identified that the position errors of the cavities, dielectric and the rotation errors of the cavities as discussed in subsection 4.4.3 can affect the sensitivity and can lead to errors in the position measurements.

A reassembly of the BPM was performed that resulted in improved $S_{beam\text{-}pickup}$ parameters at the TM_{110} mode resonance frequencies of the individual cavities but at the expense of a shift in these frequencies. This improved $S_{beam\text{-}pickup}$ was still lower than simulated values, probably due to the relatively high loss-factor of the alumina ring compared to the loss-factor used in the simulations.

The BPM prototype was reassembled before installation in the beamline with the objective to shift the Y-axis TM_{110} mode resonance frequency as close as possible to 145.7 MHz. However, the TM_{110} mode resonance frequency of the Y-axis cavities was shifted further. The beam measurements were performed in two stages; beam current sweep for given position offsets and beam position sweeps for given beam intensities but only for the X-axis cavities.

The beam current response of the two X-axis cavities was performed at two different energies: 200 MeV (position offset of 2.4 mm and 4.8 mm) and 138 MeV (position offset of 4.8 mm). The measurement results, summarized in Figure 5.6 and Figure 5.7, indicate that for a given position offset, the BPM prototype has a linear response to beam current, indicative of good agreement between actual and simulated behavior. However, for beam currents ≤ 2.5 nA, there is large uncertainty in the normalized cavity response. This could be due to the measurement-offset affecting measurements with a spectrum analyzer in this intensity range more strongly because the background and beam-induced signals are subtracted as scalars rather than vectors. Thus, for the beam position

characterization, the measurements have been performed at 2.6 nA and at 12.2 nA.

The beam position response of the two X-axis cavities was performed at a beam energy of 138 MeV. (see Figure 5.9). It has been observed that the position sensitivity of the X2 cavity is higher than the X1 cavity by approximately 32% for measurements with 2.6 nA and 29% for measurements with 12.2 nA. Similarly, the position sensitivity of the X2 cavity differs by 11% between measurements with 2.6 nA and 12.2 nA. For the X1 cavity, the difference in position sensitivity between measurements with 2.6 nA and 12.2 nA, is approximately 14%. Due to the higher position sensitivity of the X2 cavity compared to the X1 cavity, the X2 cavity has a linear response over the range -10.0 mm to +10 mm, while for the X1 cavity, the linear response is limited to the position range -10.0 mm to +3.0 mm. For a more accurate measurement of the position sensitivity of the cavities, a vector measurement of the measurement-offset, using I/Q demodulation with respect to cyclotron RF as discussed, could be helpful.

One of the important observations from the measurement is the non-excitation of the dipole mode's horizontal polarization for vertical beam displacements, which validates the dipole mode characterization in the prototype.

The position measurements with the X1 and X2 cavities have been compared with the reference position measurement. From these results, we anticipate that the cavities with their existing measurement chain and setup can achieve a position measurement with an uncertainty (1 σ) better than 0.50 mm. The detection threshold, the position error, and the position resolution can be enhanced with better isolation from RF interference, a stronger amplification, I/Q demodulation with respect to the RF of the cyclotron, and also an optimized design of the BPM.

A new BPM design has been made to deliver more signal power for a given beam offset with reduced TM_{010} mode amplitude at the TM_{110} resonance frequency. The new BPM design has a larger separation between the TM_{010} and TM_{210} modes and the TM_{110} mode, respectively, as compared to the prototype and their presence at the TM_{110} mode frequency is reduced significantly by opting for a high Q-factor compared to the prototype. The design modifications are expected to improve the position sensitivity of the new BPM design by a factor of 2.4 as compared to the previous design. For a position offset of 2 mm, the new BPM design is expected to deliver 15% higher signal (in absolute signal level), which can increase up to 44% higher with respect to the prototype for a position offset of 5 mm. These

improvements are possible only when the loss factor of the alumina ring is less than 2×10^{-4}, which has been obtained in the new rings, we recently acquired.

To our knowledge, this is the first time non-interceptive beam position measurements have been demonstrated for proton beams of energies 200 MeV and 138 MeV and for beam currents as low as 2.6 nA. With a dedicated measurement chain and a good RF isolation, position measurements for beam currents down to 0.1 nA should be possible with a measurement bandwidth of 1 Hz.

The objective of the Chapter was to demonstrate non-invasive position measurement of proton beams in a medical cyclotron beamline. This has been demonstrated successfully with a four-quadrant dielectric-filled cavity BPM.

5.7 References

[1] Rohde & Schwarz GmbH & Co. KG., "ZNB Vector Network Analyzer Specifications," 2017. https://scdn.rohde-schwarz.com/ur/pws/dl_downloads/dl_common_library/dl_brochures_and_datasheets/pdf_1/service_support_30/ZNB_dat-sw_en_5214-5384-22_v0900_96dp.pdf (accessed Mar. 09, 2020).

[2] B. Whitlock and J. Fox, "Ground loops: The rest of the story," in *129th Audio Engineering Society Convention 2010*, 2010, vol. 2, pp. 1396–1404.

[3] "FSH8 Spectrum Analyzer Operating Manual," Munich, Germany, 2020. [Online]. Available: https://www.rohde-schwarz.com/ca/manual/r-s-fsh4-8-13-20-operating-manual-manuals-gb1_78701-29159.html.

[4] E. B. Joffe and K.-S. Lock, *Grounds for Grounding*. New Jersey, 2010.

[5] "RADIOCOMMUNICATIONS IN SWITZERLAND," 2020. www.elicensing.admin.ch (accessed Mar. 04, 2020).

[6] C. Ziomek and P. Corredoura, "Digital I/Q demodulator," *Proc. IEEE Part. Accel. Conf.*, vol. 4, pp. 2663–2665, 1995, doi: 10.1109/pac.1995.505652.